Journal of Statistical Physics, Vol. 70, Nos. 3/4, 1993

Stress–Stress Correlation Functions in Lattice Gases Beyond Boltzmann's Approximation

G. A. van Velzen,[1] R. Brito,[2,3] and M. H. Ernst[2]

Received April 7, 1992

The complete time dependence of the stress–stress correlation functions in lattice gas cellular automata is calculated from the ring kinetic theory using numerical and analytical methods. This provides corrections, typically of 10–20%, to the usual molecular chaos calculations, where correlation functions decay exponentially. The resulting correlation function crosses over from an initial exponential decay to the long-time behavior calculated from mode coupling theory. The present theory, applied to the viscosity, accounts for a substantial part of the observed difference between the Boltzmann theory and simulations.

KEY WORDS: Stress correlation functions; lattice gas cellular automata; ring collisions; transport coefficients; long-time tails.

1. INTRODUCTION

In this paper we discuss the well-known lattice gas cellular automata models introduced by Frisch, Hasslacher, and Pomeau (FHP).[1] They are tailored for simulation on a computer, but they also offer a challenge to test methods of statistical mechanics and kinetic theory. One of the challenges is to explain differences of up to 40%[2–4] between the transport coefficients measured in computer simulations and those calculated from the Boltzmann equation. For instance, in the so-called FHP lattice gas models, defined on the triangular lattice, the reported values for the kinematic viscosity differ up to 40% from the predicted Boltzmann values

[1] Utrecht Biophysics Research Institute, University of Utrecht, P.O.B. 80000, 3508 TA Utrecht, The Netherlands.

[2] Institute for Theoretical Physics, University of Utrecht, P.O.B. 80006, 3508 TA Utrecht, The Netherlands.

[3] Permanent address: Facultad de Ciencias Físicas, Universidad Complutense, 28040 Madrid, Spain.

0022-4715/93/0200-0811$07.00/0

in the FHP-I model[2]; differences of 15–25% are reported in refs. 2 and 4 for the FHP-III model. Even larger differences between measurements and the Boltzmann theory have been found by Boghosian and Levermore[3] for the collective diffusion coefficient in a purely diffusive lattice gas (no momentum conservation) defined on a square lattice. On the other hand, lattice gas simulations of self-diffusion problems show an excellent agreement (within 1% at all densities) between Boltzmann values for the diffusion coefficients of tagged particles, both in two and three dimensions.[5]

The first goal of the present paper is to address this problem for the FHP models. This will be done by using the so-called *ring kinetic theory*[6, 7] to evaluate analytically and numerically corrections to the transport coefficients and compare the results with available simulation data.

A second challenge is to calculate the observed time dependence of the velocity autocorrelation function of a tagged particle for *all* times. Its time sum gives the coefficient of self-diffusion. For short times this dependence is well described by the Boltzmann equation; for long times the observed behavior[5, 8, 9, 10] is equally well explained by the mode coupling theory[11, 12] or by the ring kinetic theory.[7, 13] However, for intermediate time no theoretical predictions are available.

In the present paper we evaluate time correlation functions of microscopic stresses for all times with the help of the ring kinetic theory. We concentrate here on fluid-type functions, such as the stress–stress correlation functions in FHP models. Their time sums yield the viscosities for these models.

The paper is organized as follows. In the next section the definition of the models is given, after which (in Section 3) the expressions needed from the kinetic theory of ref. 7 are given. The long- and short-time behaviors are analyzed in Section 4 and the numerical method is described in Section 5. Finally, the results are discussed in Section 6. Some technicalities are deferred to an Appendix.

2. LATTICE GASES

A lattice gas is a collection of N particles defined on a d-dimensional regular lattice $\mathscr{L}$ with a discrete number of velocities $\mathbf{c}_i$ ($i = 1,..., b$), where b is the so-called *number of bits*. The lattice is contained in a periodic box of L_l lattice spacings in the l direction ($l = x, y,..., d$) with $V = L_x L_y \cdots L_d$ the number of lattice sites. The state of an LGCA is described by the occupation numbers $n_i(\mathbf{r}, t)$, $\mathbf{r} \in \mathscr{L}$, which take only the value 1 if the velocity channel or link i at node $\mathbf{r}$ is occupied and 0 otherwise.

In this paper we restrict ourselves to the so-called FHP models, defined on a triangular lattice with six links per node. There are several

models, depending on the collision rules and on the presence of rest particles. FHP-I has no rest particle ($b=6$) and only binary and triple collisions, and FHP-II and III have a rest particle ($b=7$). FHP-III is *self-dual*, i.e., invariant under the interchange of particles and holes. The precise definition of the collision rules can be found in ref. 2.

The time evolution of an LGCA consists of two steps: collision and propagation. The collision step is performed according to certain collision rules specified in the collision operator $I_i(n)$, which is a nonlinear function of the occupation numbers n_i. The collision rules may be deterministic or stochastic. They conserve particle number and momentum and satisfy the detailed balance condition.[1] After the collision has taken place, the propagation step follows, in which a particle at node $\mathbf{r}$ with speed $\mathbf{c}_i$ moves to $\mathbf{r}+\mathbf{c}_i$. Combination of collision and propagation step gives the *evolution equation*:

$$S_i n_i(\mathbf{r}, t+1) \equiv n_i(\mathbf{r}+\mathbf{c}_i, t+1) = n_i(\mathbf{r}, t) + I_i(n(t)) \tag{2.1}$$

where we have introduced the translation operator S_i that shifts the argument $\mathbf{r}$ in the occupation number to $\mathbf{r}+\mathbf{c}_i$. It can be represented as a $bV \times bV$ matrix with elements $S_{ij}(\mathbf{r}, \mathbf{r}') = \delta_{ij}\delta(\mathbf{r}', \mathbf{r}+\mathbf{c}_i)$. The first term on the right-hand side of Eq. (2.1) represents the propagation, the second term the collisions.

If f denotes the equilibrium average occupation number $f = \langle n_i(\mathbf{r}, t)\rangle$, the collision operator can be expanded around it as

$$I_i(n) = \sum_{\lambda=1}^{b} \frac{1}{\lambda!} \Omega^{(\lambda)}_{ii_1\cdots i_\lambda}\, \delta n_{i_1} \cdots \delta n_{i_\lambda} \equiv \Omega^{(1)}_{ij}\, \delta n_j + \Omega_i(n(t)) \tag{2.2}$$

where the fluctuations in the occupation numbers are defined as $\delta n_i(\mathbf{r}, t) \equiv n_i(\mathbf{r}, t) - \langle n_i\rangle = n_i(\mathbf{r}, t) - f$, and the equilibrium relation $I_i(f) = 0$ has been used. Repeated indices imply summation (Einstein convention). Some properties of the Ω coefficients are:

- (P1) $\Omega^{(\lambda)}_{ii_1\cdots i_\lambda}$ is symmetric in the labels $(i_1 \cdots i_\lambda)$.
- (P2) $\Omega^{(\lambda)}_{ii_1\cdots i_\lambda}$ vanishes if at least two indices out of $(i_1 \cdots i_\lambda)$ are equal.
- (P3) $\Omega^{(1)}_{ij}$ (linearized Boltzmann collision operator) is symmetric in i and j.

The ring kinetic theory of ref. 7, the results of which are summarized in the next section, is formulated in terms of the kinetic propagator Γ, defined as

$$\Gamma_{ij}(\mathbf{r}, t)\kappa = \langle \delta n_i(\mathbf{r}, t)\, \delta n_j(\mathbf{0}, 0)\rangle \tag{2.3}$$

where $\langle \cdots \rangle$ is an average over an equilibrium ensemble. It is normalized to $\delta_{ij}\delta(\mathbf{r}, \mathbf{0})$ at $t=0$, where δ_{ij} and $\delta(\mathbf{r}, \mathbf{r}')$ are the Kronecker deltas of the velocities and positions, respectively, and

$$\kappa = \langle \delta n_i \, \delta n_i \rangle = \langle n_i^2 \rangle - \langle n_i \rangle^2 = f(1-f) \tag{2.4}$$

The main object of interest in this paper is the stress–stress correlation function:

$$\phi^a(t) = \kappa^{-1} \sum_{\mathbf{r}} j_i^a \langle \delta n_i(\mathbf{r}, t) \, \delta n_j(\mathbf{0}, 0) \rangle j_j^a \tag{2.5}$$

with a normalization $j_i^a j_i^a = 1$ so that $\phi^a(0) = 1$. It can be expressed in terms of the kinetic propagator as

$$\phi^a(t) = \sum_{\mathbf{r}} j_i^a \Gamma_{ij}(\mathbf{r}, t) j_j^a = j_i^a \hat{\Gamma}_{ij}(\mathbf{0}, t) j_j^a \tag{2.6}$$

with the Fourier transform defined as $\hat{\Gamma}(\mathbf{q}) = \sum_{\mathbf{r}} \exp(-i\mathbf{q}\cdot\mathbf{r})\, \Gamma(\mathbf{r})$. The currents j^a are different, depending on the correlation function considered.

The correlation function for the shear viscosity ν contains a current

$$j^\nu = \frac{2}{\sqrt{3}} c_x c_y \tag{2.7}$$

and that for the bulk viscosity ζ contains

$$j^\zeta = (\tfrac{14}{3})^{1/2} (\tfrac{1}{2} c^2 - c_0^2) \tag{2.8}$$

Here, c_0 is the speed of sound, defined as $c_0^2 = \sum_i c_i^2 / bd$. Note that for single-speed models $c_0 = 1/\sqrt{d}$ and $j^\zeta = 0$, as is the case for FHP-I. In fact, the ϕ^a can be considered as components of a fourth-rank tensor $T_{\alpha\beta\gamma\delta} = (c_{i\alpha} c_{i\beta} - c_0^2 \delta_{\alpha\beta}) \Gamma_{ij} (c_{j\gamma} c_{j\delta} - c_0^2 \delta_{\gamma\delta})$. As a fourth-rank tensor on a triangular lattice is isotropic, it has only two independent coefficients,

$$T_{\alpha\beta\gamma\delta} = \phi^\nu \left(\delta_{\alpha\gamma}\delta_{\beta\delta} + \delta_{\alpha\delta}\delta_{\beta\gamma} - \frac{2}{d} \delta_{\alpha\beta}\delta_{\gamma\delta} \right) + \phi^\zeta \delta_{\alpha\beta}\delta_{\gamma\delta} \tag{2.9}$$

Then the correlation functions are

$$\begin{aligned} \phi^\nu &= T_{xyxy} = (T_{xxxx} - T_{xxyy})/2 \\ \phi^\zeta &= (T_{xxxx} + T_{xxyy})/2 \end{aligned} \tag{2.10}$$

The two equalities on the first line are a consequence of the isotropy of the fourth-rank tensor. The viscosities are given by the long-time limit of the following correlation function expressions[14]:

$$\nu(t) = \frac{1}{8} + \frac{1}{4} \sum_{\tau=1}^{t} \phi^{\nu}(\tau) \tag{2.11}$$

$$\zeta(t) = \frac{1}{28} + \frac{1}{14} \sum_{\tau=1}^{t} \phi^{\zeta}(\tau) \tag{2.12}$$

3. KINETIC THEORY FOR STRESS–STRESS CORRELATION FUNCTIONS

In this section we summarize the results of the ring kinetic theory of ref. 7 in so far as they are needed in the present paper. This theory derives an equation for the kinetic propagator in terms of higher-order correlation functions. Then a Gaussian approximation is applied to obtain a closed integral equation, called the *ring kinetic equation.* It will be evaluated numerically in forthcoming sections.

The propagator (2.6) is written there as

$$\hat{\Gamma}_{ij} = \hat{\Gamma}^0_{ij} + \hat{\Gamma}^0_{im} S^{-1}_m \otimes \Omega^{(2)}_{mi_1 i_2} R_{i_1 i_2, j_1 j_2} \Omega^{(2)}_{lj_1 j_2} \otimes \hat{\Gamma}^0_{lj} \tag{3.1}$$

where we have suppressed the $\mathbf{q}$ and t dependence of the operators $\Gamma(\mathbf{q}, t)$ and $R(\mathbf{q}, t)$. In this equation, $S^{-1} = \exp(-i\mathbf{q} \cdot \mathbf{c})$ is diagonal and the Boltzmann approximation for the propagator is

$$\hat{\Gamma}^0_{ij}(\mathbf{q}, t) = [S^{-1}(\mathbb{1} + \Omega^{(1)})]^t_{ij} = [e^{-i\mathbf{q}\cdot\mathbf{c}}(\mathbb{1} + \Omega^{(1)})]^t_{ij} \tag{3.2}$$

and the time convolution product is defined as

$$(f \otimes g)(t) = \sum_{\tau=0}^{t-1} f(t-1-\tau)\, g(\tau) \tag{3.3}$$

Furthermore, the ring operator is given by

$$R_{i_1 i_2, j_1 j_2}(\mathbf{q}, \tau) = \frac{\kappa}{2V} \sum_{\mathbf{k}} \hat{\Gamma}_{i_1 j_1}(\mathbf{k}, \tau)\, S^{-1}_{j_1}(\mathbf{k})\, \hat{\Gamma}_{i_2 j_2}(\mathbf{q}-\mathbf{k}, \tau)\, S^{-1}_{j_2}(\mathbf{q}-\mathbf{k}) \tag{3.4}$$

The $\Omega^{(2)}_{ijk}$ in (3.1) are the coefficients of the quadratic terms in the fluctuation expansion (2.2) of the collision operator. The structure of the ring term in (3.1) is a Boltzmann propagator (Γ^0), a collision ($\Omega^{(2)}$), two parallel full propagators (ΓS^{-1}), a recollision ($\Omega^{(2)}$), and finally a Boltzmann propagator (Γ^0). This is the normal structure of the ring collision term in

the kinetic theory of continuous fluids.[6] There are additional ring terms with 3, 4,..., $b-1$ parallel full propagators[7] that will not be considered here.

In the FHP models the currents j^a in (2.6) are eigenvectors of $\Omega^{(1)}$ with eigenvalue $(-\omega_a)$, listed in Table I. Then we can express the correlation function as

$$\phi^a(t) = \phi_0^a(t) + \sum_{\tau=1}^{t-1} \tau(1-\omega_a)^{\tau-1} B_{ij}^a R_{ij,kl}(\mathbf{0}, t-\tau-1) B_{kl}^a \tag{3.5}$$

where

$$B_{ij}^a \equiv j_k^a \Omega_{kij}^{(2)} \tag{3.6}$$

and

$$\phi_0^a(t) = (1-\omega_a)^t \tag{3.7}$$

In all formulas the summation convention is used. The first term on the right-hand side of Eq. (3.5) is the Boltzmann part ϕ_0^a of the correlation function, which *only* takes into account uncorrelated collisions. In the literature, only this term has been considered. It decays exponentially, while the actual decay of the correlation function is algebraic. Nevertheless, the Boltzmann approximation gives predictions for transport coefficients that agree with computer simulations within 1% for the diffusion coefficient at all densities[5] and from 15 to 25% for the viscosities.[2,4]

As a further simplification, we replace R in Eq. (3.5) by R^0, where R^0 is given by the right-hand side of Eq. (3.4) with the full kinetic propagator $\hat{\Gamma}(\mathbf{q}, \tau)$ replaced by its Boltzmann value $\hat{\Gamma}^0(\mathbf{q}, \tau)$. In this approximation, we are ignoring collision sequences that contain *rings within rings*. Equation (3.5) with $R_{ij,kl}^0$ is the starting point of this paper. It will be evaluated *numerically*. The results show a crossover from exponential to algebraic time decay in the correlation function and give a correction to the Boltzmann values for the transport coefficients. In the next section two limiting cases for long and short times will be studied *analytically*.

TABLE I. Eigenvalues of Boltzmann Collision Operator, $\Omega^{(1)} j^a = -\omega_a j^a$, for FHP Models[15]

	FHP-I	FHP-III
ω_ν	$3f(1-f)^3$	$\kappa(7-8\kappa)$
ω_ζ	0	$7\kappa(1-2\kappa)$

4. LONG- AND SHORT-TIME ANALYSIS

4.1. Long Times

Consider first the long-time behavior of the correlation function. As has been shown in ref. 7, the ring integral $R(\mathbf{q}, t)$ has a slow algebraic decay $t^{-d/2}$, while $(1-\omega_a)^t$ has a fast exponential decay. Hence, for times large compared with a characteristic relaxation time of the order of $1/\omega_a$, the ring integral $R^0(\mathbf{0}, t-\tau-1)$ in Eq. (3.5) can be approximated by $R^0(\mathbf{0}, t)$ and we can perform the τ summation, giving $1/\omega_a^2$. Then, at long times, the correlation function becomes

$$\phi^a(t) \simeq \frac{1}{\omega_a^2} B_{ij}^a R_{ij,kl}^0(\mathbf{0}, t) B_{kl}^a \tag{4.1}$$

If $a^\mu(\mathbf{q})$, with components $a_i^\mu(\mathbf{q}) = a^\mu(\mathbf{q}, \mathbf{c}_i)$, denotes an eigenvector and $e^{z_\mu(q)}$ the corresponding eigenvalue of the Boltzmann kinetic propagator $\hat{f}^0$, then

$$\hat{f}^0 a^\mu(\mathbf{q}) = e^{-i\mathbf{q}\cdot\mathbf{c}}(\mathbb{1} + \Omega^{(1)})\, a^\mu(\mathbf{q}) = e^{z_\mu(q)} a^\mu(\mathbf{q}) \tag{4.2}$$

The spectrum of $\hat{f}^0$ contains b modes (with $b=6$ or 7 in the FHP models), three of which are slow or hydrodynamic modes; one of them is related to number and two to momentum conservation. In particular, there are two sound modes $\sigma = \pm$ with eigenvalue $z_\sigma(q) = ic_0\sigma q - \frac{1}{2}\gamma q^2$ as $\mathbf{q} \to 0$ and one shear mode with $z_\nu(q) = -\nu q^2$. The remaining $(b-3)$ modes are fast or kinetic modes, with nonzero eigenvalue as $\mathbf{q} \to 0$. Here, γ is the sound damping constant. It can be expressed in terms of the shear and bulk viscosity as $\gamma = \nu + \zeta$. Making a spectral decomposition of $\hat{f}^0$ in the expression for the ring integral (3.4) gives (see ref. 7 for details)

$$R_{ij,kl}^0(\mathbf{k}, t) = \frac{\kappa}{2V} \sum_{\mathbf{q}} \sum_{\mu\nu} a_i^\mu(\mathbf{q})\, a_j^\nu(\mathbf{k}-\mathbf{q}) \times \exp[z_\mu(q)t + z_\nu(|\mathbf{k}-\mathbf{q}|)t]\, a_k^\mu(\mathbf{q})\, a_l^\nu(\mathbf{k}-\mathbf{q}) \tag{4.3}$$

A peculiarity of the FHP models is the occurrence of three additional soft modes, due to the conservation of staggered momentum. These staggered modes become soft at finite $\mathbf{k}$ values, given by the corners of the Brillouin zone. These soft modes should also be included in the $\mathbf{k}$ summation of (4.3).[11] As we are interested in the long-time behavior, only the slowest decay rates, corresponding to the soft modes, are of relevance. Then, the sum on μ, ν runs only over soft modes. In addition we use the property[7]

$$\Omega_{ijk}^{(2)} a_j^\mu a_k^\nu = -\frac{1-2f}{\kappa} \Omega_{ij}^{(1)} a_j^\mu a_j^\nu \tag{4.4}$$

which holds for all collision rules, and we obtain the basic equation of the *mode coupling theory*,

$$\phi^a(t) \simeq \frac{1}{2V} \sum_{\mathbf{q}} \sum_{\mu\nu} |A^a_{\mu\nu}(\mathbf{q})|^2 \, e^{[z_\mu(q) + z_\nu(q)]t}$$
$$A^a_{\mu\nu}(\mathbf{q}) = \frac{1-2f}{[f(1-f)]^{1/2}} \sum_i j^a_i a^\mu_i(\mathbf{q}) \, a^\nu_i(-\mathbf{q}) \tag{4.5}$$

The amplitudes $A^a_{\mu\nu}(\mathbf{q})$ have the standard form of mode coupling theory, i.e., a projection of a current j^a on a product of two hydrodynamic modes $a^\mu(\mathbf{q})\, a^\nu(-\mathbf{q})$. Not only does Eq. (4.5) yield in the thermodynamic limit the dominant $1/t$ tail of two-dimensional time correlation functions,[11] but the discrete $\mathbf{q}$ summation also accounts in an excellent way for finite-size effects.[9] The dominant *long-time tail* for the transverse stress–stress correlation function reads explicitly

$$\phi^\nu(t) \simeq \frac{2^{-8}}{\pi\sqrt{3}} \frac{(1-2f)^2}{f(1-f)} \left[\frac{1}{\nu} + \frac{1}{\gamma} + \frac{3}{(\xi_1 \xi_2)^{1/2}} \right] \frac{1}{t} \tag{4.6}$$

with ξ_1, ξ_2 the longitudinal and transverse diffusivities of the staggered momentum modes of the FHP models.[15] The longitudinal stress–stress correlation function has a dominant tail given by $\phi^\zeta(t) = \frac{4}{7}\phi^\nu(t)$. The algebraic t^{-1} tail in (4.6) implies that the transport coefficients (2.11) and (2.12) diverge logarithmically. This is the well-known problem of the nonexistence of two-dimensional hydrodynamics. We will return to this problem later.

4.2. Short Times

The behavior of $\phi^a(t)$ can be obtained not only for long times, but also for short ones. For $t = 0, 1$ only the Boltzmann part is present in (3.5), because the convolution sum runs from $\tau = 1$ to $t-1$, i.e., the sum is empty. For $t = 2$, the sum in (3.4) is evaluated at $\tau = 1$, where

$$R^0_{i_1 i_2, j_1 j_2}(\mathbf{0}, 0) = \frac{\kappa}{2V} \sum_{\mathbf{k}} \exp[-i\mathbf{k} \cdot (\mathbf{c}_{j_1} - \mathbf{c}_{j_2})] \delta_{i_1 j_1} \delta_{i_2 j_2}$$
$$= \frac{\kappa}{2} \delta(\mathbf{c}_{j_1}, \mathbf{c}_{j_2}) \delta_{i_1 j_1} \delta_{i_2 j_2} = 0 \tag{4.7}$$

The relation $\hat{\Gamma}^0_{ij}(\mathbf{0}, 0) = \delta_{ij}$ has been used [see below (2.3)]. The delta condition has to be satisfied with $\mathbf{c}_{j_1} \neq \mathbf{c}_{j_2}$ on account of the property P2.

This is impossible in regular geometries, i.e., in systems contained in a macroscopic periodic cell which is more than two lattice spacings wide in all directions. Hence $R(\mathbf{0}, 0) = 0$. However, in *slab* geometries[16] in which at least one dimension has been set equal to 2, the condition (4.7) can be fulfilled *through the periodic boundary.* This is the origin of the non-vanishing contribution to the correlation functions. There are no dynamical correlations in regular geometries at $t = 1, 2$, because the minimum time to produce a recollision is three time steps.

Next we consider the ring integral (3.4) for general t values, and replace Γ by Γ^0 in (3.2) and set $\mathbf{q} = 0$. With the help of the relation

$$V^{-1} \sum_{\mathbf{k}} \exp[i\mathbf{k} \cdot (\mathbf{c} - \mathbf{c}')] = \delta(\mathbf{c}, \mathbf{c}') \tag{4.8}$$

we obtain

$$\begin{aligned} R^0_{ij,kl}(\mathbf{0}, t) = \frac{\kappa}{2} (\mathbb{1} + \Omega^{(1)})_{ik_1} (\mathbb{1} + \Omega^{(1)})_{k_1 k_2} \cdots (\mathbb{1} + \Omega^{(1)})_{k_{t-1} k_t} \\ \times (\mathbb{1} + \Omega^{(1)})_{jl_1} (\mathbb{1} + \Omega^{(1)})_{l_1 l_2} \cdots (\mathbb{1} + \Omega^{(1)})_{l_{t-1} l_t} \\ \times \delta(\mathbf{c}_i + \mathbf{c}_{k_1} + \mathbf{c}_{k_2} + \cdots + \mathbf{c}_{k_t}, \mathbf{c}_j + \mathbf{c}_{l_1} + \mathbf{c}_{l_2} + \cdots + \mathbf{c}_{l_t}) \end{aligned} \tag{4.9}$$

with $k_t = k$, $l_t = l$. The delta function is nonvanishing if the velocities form a closed polygon. This is the ring condition, expressing that the two particles under consideration have to be in the same node at the initial ($t = 0$) and final time t. The ring integral $R(\mathbf{0}, t)$ contains in principle b^{2t} terms, and we have not been able to evaluate the general term. Here we only show the explicit calculation of $R^0(\mathbf{0}, 1)$. This result has been used to test our computer code.

To have a nonvanishing contribution to (4.9), we have to guarantee that $i \neq j$ and $k \neq l$, because $B^a_{ij} = 0$ for $i = j$ in (3.6) on account of property P2. Below we will analyze the condition $\mathbf{c}_i + \mathbf{c}_k = \mathbf{c}_j + \mathbf{c}_l$ for the simplest model, FHP-I, without a rest particle. Consider Fig. 1. The different possibilities in the absence of a rest particle are shown in Figs. 1a–1c. For fixed $\mathbf{c}_i$ there are two diagrams of type (a), two diagrams of type (b), and five diagrams of type (c). The conditions in Fig. 1 can be summarized as $i \neq j$ and

$$\delta(\mathbf{c}_i + \mathbf{c}_k, \mathbf{c}_j + \mathbf{c}_l) = \delta_{il}\delta_{kj} + \delta_{i,k+3}\delta_{j,l+3} - \delta^{(4)}_{i,j+3,k+3,l} \tag{4.10}$$

The symbol $\delta^{(4)}$ on the right-hand side is equal to 1 if all the indices are equal, and 0 otherwise. It corrects for double counting of trajectories. The extension of condition (4.10) when rest particles are involved can be constructed in a straightforward manner from the diagrams in Figs. 1e and 1d, but will not be written down.

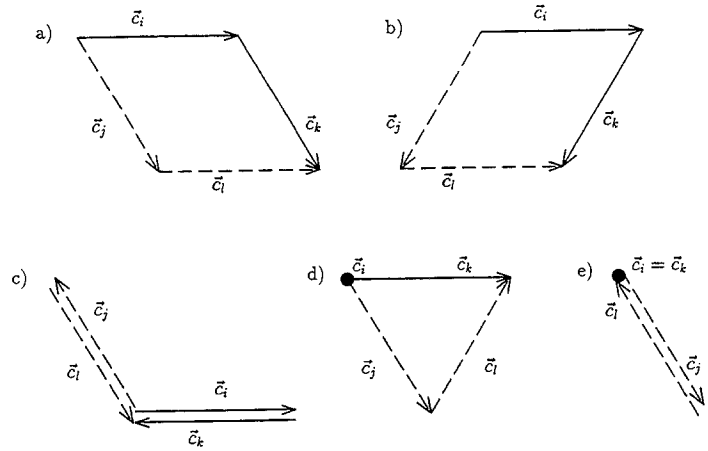

Fig. 1. Ring collision in $R(t=1)$ in FHP models involving two time steps, satisfying the ring condition $\mathbf{c}_i+\mathbf{c}_k=\mathbf{c}_j+\mathbf{c}_l$ $(i\neq j;\ k\neq l)$. Diagrams (a), (b), (c) only involve moving particles; (d) and (e) involve a rest particle, denoted by ●.

Next we need to evaluate the coefficients B^a_{ij} defined in Eq. (3.6) in terms of the coefficients $\Omega^{(2)}_{ij_1j_2}$. These coefficients are calculated in the Appendix. As FHP-I is a single-speed model, the correlation function for the bulk viscosity has a vanishing current [see (2.8)]. The only relevant correlation function is the one related to the shear viscosity, with a current

$$j^\nu=\frac{2}{\sqrt{3}}c_xc_y=\frac{1}{2}(0,\ 1,\ -1,\ 0,\ 1,\ -1) \tag{4.11}$$

The matrix B^ν follows after a lengthy calculation from (3.6) and (A3) in the Appendix, with the result

$$B^\nu=\begin{pmatrix} 0 & a & -a & 0 & a & -a \\ a & 0 & 0 & a & -b & 0 \\ -a & 0 & 0 & -a & 0 & b \\ 0 & a & -a & 0 & a & -a \\ a & -b & 0 & a & 0 & 0 \\ -a & 0 & b & -a & 0 & 0 \end{pmatrix} \tag{4.12}$$

where

$$a=\tfrac{3}{2}f(1-f)^2, \qquad b=\tfrac{3}{2}(1-f)^2\,(1-2f) \tag{4.13}$$

It satisfies the relation $B^\nu_{ij}=B^\nu_{i+3,j+3}$.

Finally, we need in (4.9) the values of the Boltzmann collision operator $\Omega^{(1)}$ for FHP-I. Its general expression can be found in the Appendix. We quote here only the independent elements; the remaining ones can be obtained using symmetry properties:

$$\begin{aligned} \Omega^{(1)}_{ii} &= -2c-d; & \Omega^{(1)}_{i,i+3} &= -2c+d \\ \Omega^{(1)}_{i,i+1} &= \Omega^{(1)}_{i,i+5} = c+d; & \Omega^{(1)}_{i,i+2} &= \Omega^{(1)}_{i,i+4} = c-d \\ c &= \tfrac{1}{2}f(1-f)^3; & d &= f^2(1-f)^2 \end{aligned} \tag{4.14}$$

The coefficients c and d are the contributions to $\Omega^{(1)}$ coming from binary and triple collisions, respectively. Inserting (4.10) and (4.12) into Eq. (4.9) and Eq. (3.5) for $t=3$, we obtain, after some algebra,

$$\phi^{\nu}(3) = \phi^{\nu}_0(3) + 8\kappa[a^2(5c^2+2d^2-4dc) + \tfrac{1}{4}b^2(2c-d)^2] \tag{4.15}$$

A similar analysis for the FHP-III model gives

$$\begin{aligned} \phi^{\nu}(3) &= \phi^{\nu}_0(3) + \tfrac{1}{4}\kappa^2(1-2f)^2 \\ &\quad \times (2224\kappa^5 - 4620\kappa^4 + 3595\kappa^3 - 1340\kappa^2 + 246\kappa - 16) \end{aligned} \tag{4.16}$$

$$\begin{aligned} \phi^{\zeta}(3) &= \phi^{\zeta}_0(3) + \tfrac{7}{4}\kappa^2(1-2f)^2 \\ &\quad \times (1264\kappa^5 - 2304\kappa^4 + 1498\kappa^3 - 458\kappa^2 + 69\kappa - 4) \end{aligned} \tag{4.17}$$

where $\phi^{\nu}(t)$ and $\phi^{\zeta}(t)$ are, respectively, the correlation functions related to the shear and bulk viscosity. Notice the overall factor of $(1-2f)^2$ appearing in the excess correlation functions in Eq. (4.17) for the model FHP-III. It implies that it vanishes for a half-filled lattice, where $f=1/2$. This is a typical effect present in *self-dual* models. The factor $(1-2f)$ originates from the coefficients B^a_{ij} for FHP-III, as defined in Eq. (3.5). Then, the ring corrections to the Boltzmann value are vanishing for $f=1/2$. Only higher-order diagrams may be present in this case, so that deviations from the Boltzmann result are expected to be small. We recall from (4.5) that the *long-time* behavior of the ring integral for the stress–stress correlations is proportional to $(1-2f)^2$ in *all* lattice gas models. The ring contribution to the correlation functions at $t=3$, $\phi^{\nu}_R(3) \equiv \phi^{\nu}(3) - \phi^{\nu}_0(3)$, represents at most about 1% of the Boltzmann value for the FHP-I model. However, in the FHP-III model something peculiar happens to the Boltzmann correlation function ϕ^{ν}_0. In a large density interval, $f_0 < f < 1-f_0$ with $f_0 \simeq 0.23$, the correlation function oscillates around zero with an exponentially decreasing amplitude $|1-\omega_{\nu}|^t$, where $1<\omega_{\nu}<2$. Exactly at the densities f_0 and $1-f_0$ the correlation function $\phi^{\nu}_0(t)=0$ for *all* times $t \geqslant 1$. This is illustrated in Fig. 2b, where the Boltzmann correlation $\phi^{\nu}_0(3)$ as well as the ring contribu-

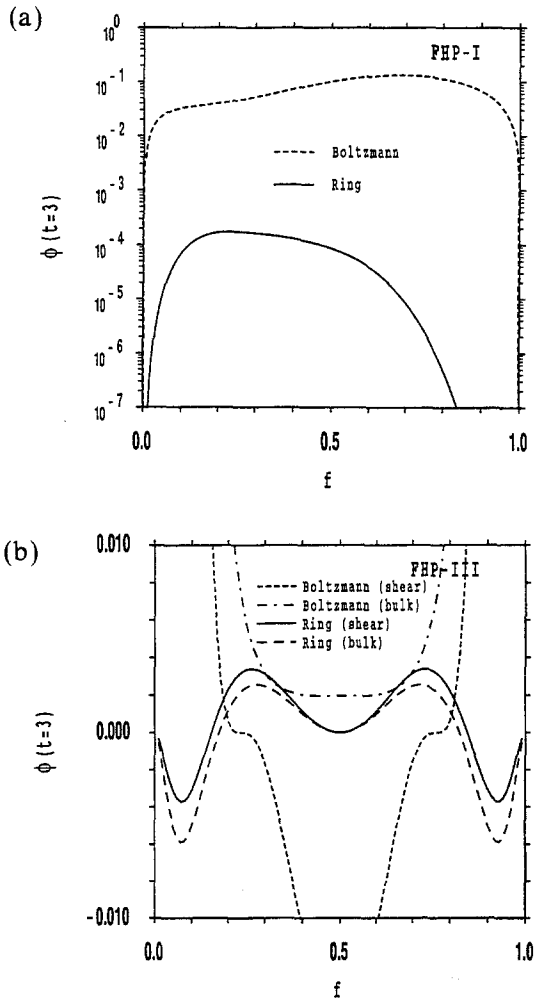

Fig. 2. Stress–stress correlation function at $t=3$: Boltzmann $[\phi_0^{\nu}(3)]$ and ring $[\phi_R^{\nu}(3)]$ in (a) FHP-I and (b) FHP-III. Note that $\phi_0^{\nu}(3)<0$ in (b) for $f_0<f<1-f_0$ ($f_0\simeq 0.23$), indicating an oscillating Boltzmann correlation function.

tion (3.5), $\phi_R^{\nu}(3)\equiv\phi^{\nu}(3)-\phi_0^{\nu}(3)$, are plotted as a function of the density. Close to f_0 and $1-f_0$ the ring contribution is larger than the Boltzmann term.

5. NUMERICAL CALCULATIONS

The analytical scheme of Section 4.2 for calculating $\phi(t)$ at general t values does not seem feasible because the number of possible trajectories

grows as b^{2t}. Following a different strategy, we have developed a numerical scheme to calculate the correlation function. It is a calculation that grows linearly with the time t. The main computational task is to evaluate R^0 by means of the $\mathbf{k}$ summation in (3.4) at $\mathbf{q}=\mathbf{0}$, where the propagators take their Boltzmann values (3.2). In the thermodynamic limit $V\to\infty$, this summation can be replaced by an integral over the first Brillouin zone: $(1/V)\sum_{\mathbf{k}}\to(2\pi)^{-2}\int_{1BZ}d\mathbf{k}$. We have calculated this integral numerically. The approach is straightforward. First the integral is written as a sum over Gaussian integration points in $\mathbf{k}$-space, whose contributions have to be summed with their corresponding Gaussian integration weights. For every $\mathbf{k}$, we calculate the $b\times b$ matrix $S^{-1}(\mathbb{1}+\Omega^{(1)})$. This is simply multiplied t times to give the Boltzmann propagator (3.2). As this is laborious for large t values, a different approach is followed here. It is based on t values that are powers of 2. The "gaps" are filled in linearly with results for lower t values, yielding data for $t=2^p+i2^{p-r}$, $i=0,\ldots,2^r-1$, $p=0,1,\ldots$. It is clear how the matrix multiplications have to be carried out. It turns out that for $r=2$ this yields sufficiently smooth curves on log-log plots. The same is done for $-\mathbf{k}$. The $(\mathbf{k})(-\mathbf{k})$ products in (3.4) are multiplied with their corresponding weight and summed to yield the integral. No use has been made of model-dependent symmetries, except for the space reflection symmetry. The latter implies that the total result is four times the real part of that of the first quadrant. We thus arrive at a $b\times b\times b\times b$ array R_{ijkl} ($b=6$ or 7), which depends only on t. Finally, we perform the contraction with the $\Omega^{(2)}$ and the currents j in (3.6). As a check, we also calculated the correlation functions $j^x\hat{\Gamma}(\mathbf{0},t)j^x$, $j^y\hat{\Gamma}(\mathbf{0},t)j^y$, and $j^x\hat{\Gamma}(\mathbf{0},t)j^y$, with $j^x=c_xc_x$ and $j^y=c_yc_y$. They are linearly related to the shear viscosity correlation function [as can be concluded from Eq. (2.9)].

As the shear, sound, and staggered modes fall off typically as $\exp(-k^2t)$, for long times the main contribution comes from points close to the origin of the Brillouin zone. For this reason we split up the integration of the first quadrant into five parts, as illustrated in Fig. 3. For convenience we write k_x, k_y as x, y. The integral is then first split up into three parts:

$$\int_{\text{1st quadrant}} R(x,y)=\int_{x=0}^{x_1}\int_{y=0}^{x\sqrt{3}}R(x,y)\,dy\,dx+\int_{y=0}^{y_1}\int_{x=0}^{y/\sqrt{3}}R(x,y)\,dx\,dy$$
$$+\int_{x_1}^{2x_1}\int_{y=0}^{2y_1-x\sqrt{3}}R(x,y)\,dy\,dx \tag{5.1}$$

where $x_1=\frac{2}{3}\pi$, $y_1=\frac{2}{3}\pi\sqrt{3}$. Consider, for instance, the first term. There we take, for every x, the N Gaussian integration points in the range from $y=0$ up to $y=\sqrt{3}\,x$. The x themselves take on N values from 0 up to x_1. The

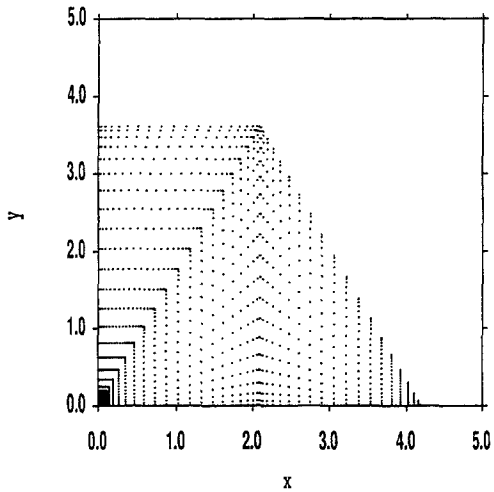

Fig. 3. Distribution of Gaussian integration points. The five parts of the integrals (5.1) and (5.2) are easily recognized. In this example there are 20×20 points in each part.

third term is not relevant for long times, so it does not need a special treatment. The density of integration points in the y direction in the first (second) term is thus inversely proportional to the value of x (y), improving the accuracy near the origin. This is further improved by splitting up the first term on the right-hand side of (5.1) as

$$\int_{x=0}^{x_1} \int_{y=0}^{x\sqrt{3}} R(x, y)\, dy\, dx = \int_{x=0}^{x_2} \int_{y=0}^{x\sqrt{3}} R(x, y)\, dy\, dx + \int_{x=x_2}^{x_1} \int_{y=0}^{x\sqrt{3}} R(x, y)\, dy\, dx \qquad (5.2)$$

Similarly we split up the second term of Eq. (5.1). The relative "accuracy" of the small-**k** region is then inversely proportional to the values x_2 and y_2. These parameters are varied in order to stabilize the calculation. A typical value we used is $x_2/x_1 = y_2/y_1 = 0.15$. In Fig. 3 we show the distribution of integration points with 20×20 points for each of the five parts. We typically use 100 times 100 integration points for each of the five parts of the integral. This is the rather straightforward method by which we obtained the results of the present paper. There may, however, be other than Gaussian integration algorithms that are even better tailored for the typical form of the integrand at long times. Here we are mostly interested in intermediate times.

Once we have obtained the ring integral $R^0_{ij,kl}(\mathbf{0}, \tau)$, it is contracted with the B^a_{ij} given in Eq. (3.6), according to Eq. (3.5). Next the convolution

sum in (3.5) is carried out to yield the time correlation functions. Finally, the transport coefficients are calculated using the Green–Kubo expressions (2.11) and (2.12).

6. RESULTS AND DISCUSSION

In this section we present the results of the numerical integration of the ring integral equation (3.5) following the scheme proposed in the previous section. We will show the crossover from the exponential Boltzmann decay to the algebraic mode coupling tails ($1/t$), as well as higher-order tail corrections $\sim(1/t^2)$. The contributions from the ring integral to the transport coefficients are also discussed.

The typical behavior of $\phi(t)$ is presented in Fig. 4 for model FHP-I at the reduced density $f=1/4$, where the eigenvalue $\omega_v=3f(1-f)^3$ is at its maximum, $\omega_v\simeq 0.316$. The mean free time is $t_m\simeq 1/\omega_v^0\simeq 3.16$. It shows clearly the two regimes already mentioned. At short times ($t\lesssim 5t_m$) the Boltzmann contribution to the correlation function is the dominant part. At intermediate times ($5t_m\lesssim t\lesssim 15t_m$) the effect of correlated collisions starts to show up, producing deviation from the Boltzmann result. For $t>20t_m$ the correlation function is completely dominated by the ring collisions and $\phi(t)$ approaches to the mode coupling result.

In Fig. 5 the Boltzmann contribution $\phi_0^a(t)$ and the ring contribution $\phi_R^0(t)=\phi^a(t)-\phi_0^a(t)$ in Eq. (3.5) are plotted separately for shear ($a=v$) and bulk viscosity ($a=\zeta$) in FHP-III at reduced density $f=1/7$, where the

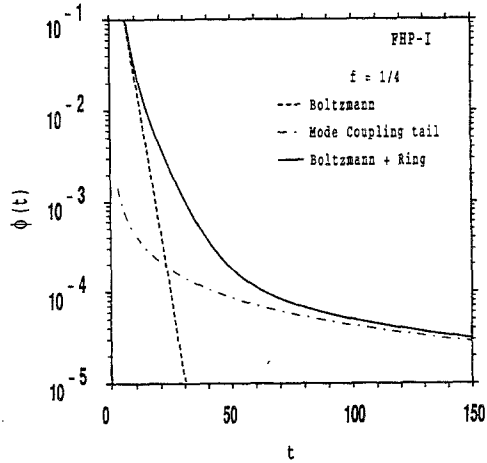

Fig. 4. Total correlation function $\phi^v=\phi_0^v+\phi_R^v$ versus time in FHP-I at reduced density $f=1/4$, where $t_m\simeq 3.16$. The dashed line represents the Boltzmann contribution ϕ_0^v and the dashed-dotted line the mode coupling $1/t$ tail.

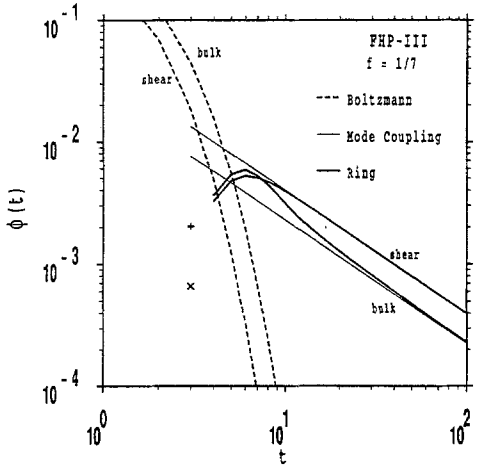

Fig. 5. Correlation function $\phi^a(t)$ for $a = v, \zeta$ in FHP-III at $f = 1/7$, where $t_m \simeq 1.4$. The ring contribution $\phi^v_R(t)$ is compared with Boltzmann $\phi^v_0(t)$ and mode coupling results. The + and × indicate the *negative* values of $\phi^\zeta_R(t=3)$ and $\phi^v_R(t=3)$, respectively.

mean free path is typically $t_m = 1/\omega_v \simeq 1.4$. Crossover from exponential to algebraic decay typically occurs between $5t_m$ and $8t_m$. Beyond $15t_m$ the correlation functions in FHP-III are completely dominated by the mode coupling (MC) results. We also observe that the mean free time in FHP-I at this density is almost 3 times larger than in FHP-III. The reason is that there are more collisions allowed in FHP-III than in FHP-I.

We further observe in Fig. 5 that $\phi^a_R(t)$ in Eq. (3.5) vanishes for $t = 1$ and $t = 2$. Note that for this density $\phi^a_R(t=3)$ is negative. It reaches a maximum at $t = 6$ and starts to approach the MC tail either from below or from above, depending on the type of function ($a = v, \zeta$) or the model (FHP-I, III) considered.

Next, we will analyze the subleading corrections to the $1/t$ tail. In order to do so, we make an asymptotic expansion of the correlation function in powers of $1/t$:

$$\phi(t) = \frac{A}{t} + \frac{B}{t^2} + \cdots \tag{6.1}$$

The first term in this expansion, A/t, has been shown both analytically (Section 4.1) and numerically (Figs. 4 and 5) to be the mode coupling result. There are no theoretical predictions for B. To obtain the coefficient B, we subtract $\phi_{MC}(t) = A/t$, multiply by t^2, and take the limit $t \to \infty$. The results are shown in Fig. 6 (FHP-I, $f = 1/4$), Fig. 7 (FHP-III, $f = 1/7$), and Fig. 8 (FHP-III, $f = 2/7$).

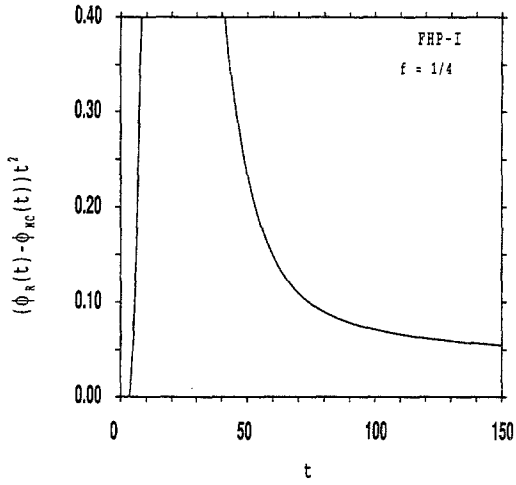

Fig. 6. Subleading tail $\sim t^{-2}$ in FHP-I at $f = 1/4$.

As the dominant term of all correlation functions is $1/t$, Eqs. (2.11) and (2.12) yield a logarithmically diverging transport coefficient when $t \to \infty$, and hydrodynamics *does not exist* in two dimensions. However, in finite systems or at moderately large times, transport coefficients remain bounded. We have plotted the time-dependent shear and bulk viscosity, as defined in Section 2, for model FHP-I (Fig. 9, $f = 1/4$) and for model

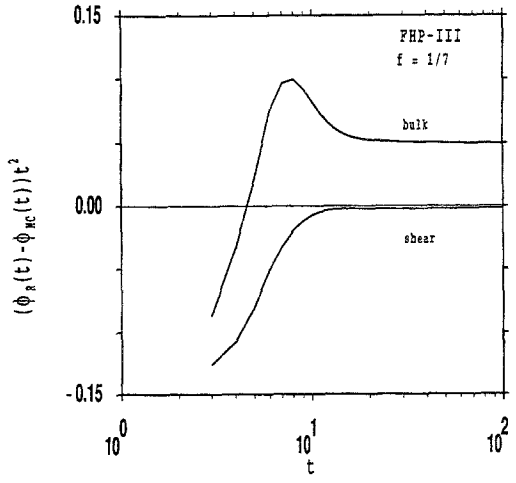

Fig. 7. Subleading tail $\sim t^{-2}$ in FHP-III at $f = 1/7$.

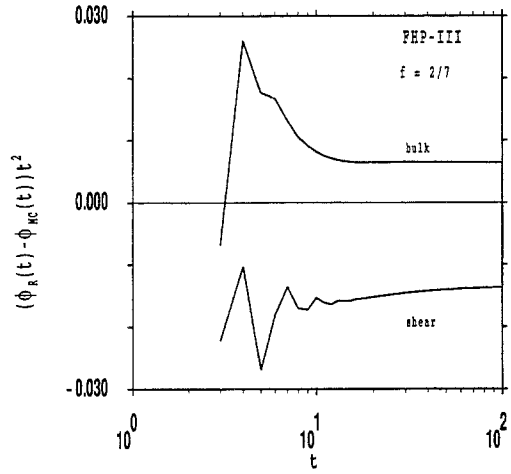

Fig. 8. Subleading tail $\sim t^{-2}$ in FHP-III at density $f = 2/7$, where $\phi_0^{\nu}(t)$ oscillates.

FHP-III (Fig. 10, $f = 1/7$). The Boltzmann contribution $\nu_0(t)$ (dashed) approaches its long-time value exponentially fast. The ring contribution (2.11) with $\phi^{\nu}(t)$ from Eq. (4.6) increases logarithmically for long times, i.e., $\nu_R(t) \sim \log t$.

In Fig. 11 we compare the data from the present theory (crosses) with the Boltzmann values. As present theory we take the Boltzmann value and

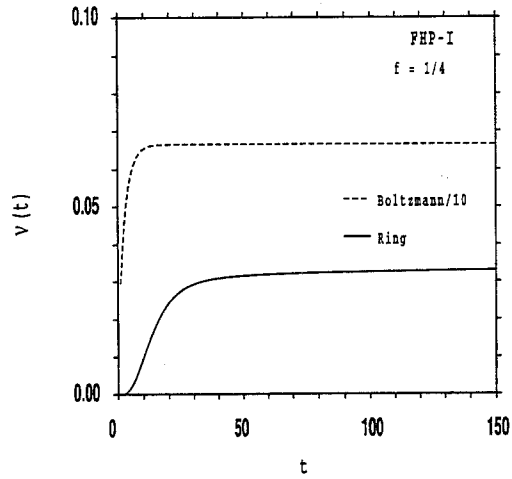

Fig. 9. Time-dependent shear viscosity in FHP-I at $f = 1/4$. Boltzmann $[\nu_0(t)]$ and ring $[\nu_R(t) \sim \log t]$ results.

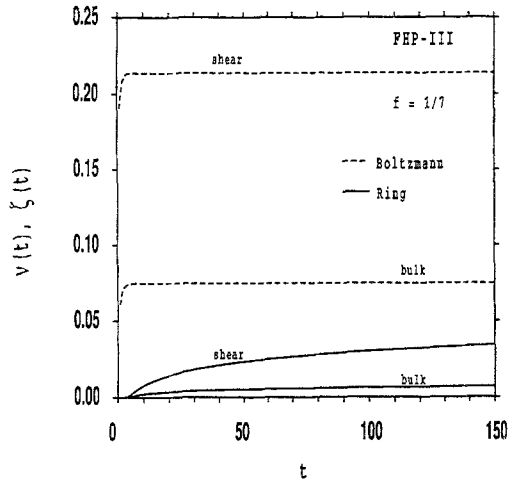

Fig. 10. Time-dependent shear and bulk viscosity in FHP-III at $f = 1/7$. Boltzmann (ν_0, ζ_0) and ring (ν_R and ζ_R) results.

add the ring part at $t = 150$. The ring contribution to the transport coefficient increases only slowly with time. From 150 to about 500 time steps $\nu_R(t) + \nu_0$ increases only about 3 or 4%.

Finally it is of interest to compare our results with those from computer simulations. For the stress–stress correlation function no simulation data are available. However, for the shear viscosity, simulation data have been given by d'Humières and Lallemand.[2] The same data for FHP-III with higher statistical accuracy were recently obtained by Gerits and Van der Hoef.[4] These authors measured the relaxation of a transverse sinusoidal flow field that decays as $\exp(-\nu k^2 t)$. They also measured the decay of a sound wave; the bulk viscosity ζ follows from the sound damping constant through $\gamma = \nu + \zeta$. The time scales involved in these measurements do not extend beyond 300 time steps. Therefore, we compare our results for the shear and bulk viscosities $[\nu_R(150) + \nu_0$ and $\zeta_R(150) + \zeta_0]$ with their simulation data (see Figs. 11a and 11b, respectively). It shows that the ring approximation for the shear viscosity accounts for more than 60% of the difference between Boltzmann and simulation results. The remaining difference comes from more complicated collisions. Also for the bulk viscosity, the present theory seems to account for the major part of the difference between Boltzmann and simulation results (see Fig. 11b).

In summary, we have numerically studied the contribution of the simplest type of correlated collisions in lattice gases: ring collisions. The numerical results show the crossover from Boltzmann decay to mode coupling tails and coincide with the numerical results in both limiting

cases: Boltzmann at short times and mode coupling at long times. Also, it accounts for most of the difference between the Boltzmann transport coefficients and their simulated values in FHP-III. The remaining difference originates from more complicated correlated collision sequences. A preliminary calculation of diagrams with additional parallel propagators at $t = 3$ shows a very small correction to the present result. It is not clear how the situation is for larger t.

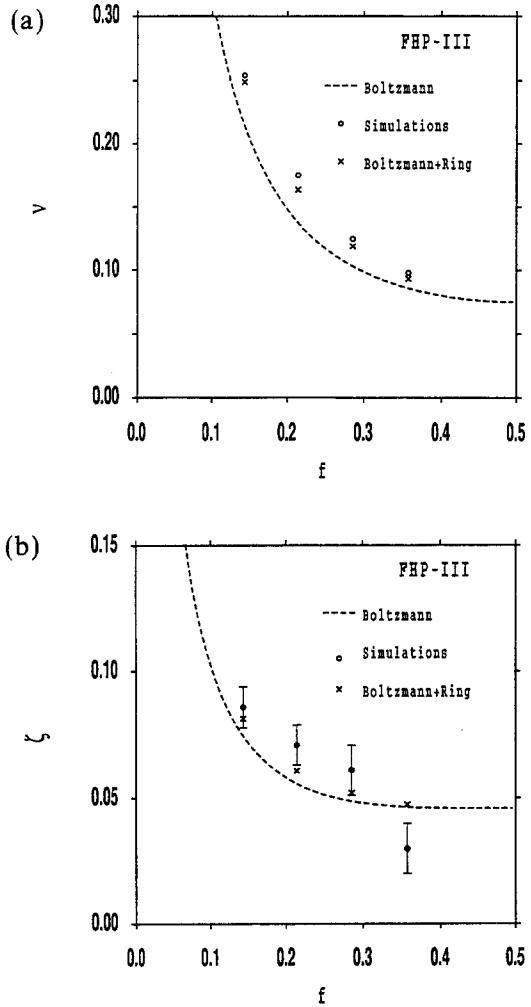

Fig. 11. Transport coefficients in FHP-III from Boltzmann, ring at $t = 150$, and simulation[4] results. (a) Shear viscosity ν: ν_0, $\nu_0 + \nu_R(150)$ and ν_{sim}; (b) bulk viscosity ζ: ζ_0, $\zeta_0 + \zeta_R(150)$, and ζ_{sim}.

We are presently considering generalization to the tagged-particle problem,[13] in particular to the velocity autocorrelation function (VACF). It is straightforward to adapt the numerical calculation described above to the tagged-particle problem: one of the two fluid propagators in Eq. (3.4) has to be replaced by the tagged-particle propagator.

The tagged particle problem derives its special interest from the fact that very accurate simulation data for the VACF are available for short, intermediate, and long times.[5, 9, 10] A comparison would make it possible to decide whether the simple ring integral in Eq. (3.4) with two parallel propagators does account quantitatively for most of the *short* and *intermediate* time behavior of the VACF, or whether rings with more parallel propagators have to be taken into account.

Of course, the long-time behavior of the simple ring fully accounts for the simulated long-time tail and for the mode coupling theory, as demonstrated in ref. 13.

APPENDIX. EVALUATION OF $\Omega^{(\lambda)}$

In this Appendix we give general expressions for the coefficients $\Omega^{(\lambda)}$ defined in (2.2), in terms of the basic transition probabilities that define the nonlinear collision operator $I_i(n)$ in Eq. (2.1). Let $A_{s\sigma}$ denote the transition probability from the input state s to the input state σ; then the collision operator can be written as

$$I_i(n) = \sum_{\sigma s} (\sigma_i - s_i) A_{s\sigma} \prod_k n_k^{s_k} (1-n_k)^{(1-s_k)} \tag{A1}$$

For an explicit definition of states s and σ and transition probabilities we refer to ref. 1. We recall that s_i, s_k, σ_i, n_k $(k = 1, 2, \ldots, b)$ are Boolean variables. A convenient starting point for the fluctuation expansion of $I_i(n) = I_i(f + \delta n)$ around equilibrium is the *identity*, valid for Boolean variable s_j:

$$n_j^{s_j}(1-n_j)^{1-s_j} = f^{s_j}(1-f)^{1-s_j}\left(1 + \frac{\delta s_j\, \delta n_j}{\kappa}\right) \tag{A2}$$

with $\kappa = f(1-f)$, $\delta s_j = s_j - f$, and $\delta n_j = n_j - f$. Inserting (A2) into (A1) gives a sum of products of an increasing number of δn's. The first term vanishes because $I_i(f) = 0$. Comparing this expansion with the defining equation (2.2) allows us to identify

$$\kappa \Omega_{ij}^{(1)} = \sum_{\sigma s} (\delta\sigma_i - \delta s_i) A_{s\sigma} F_0(s)\, \delta s_j = \kappa \delta_{ij} + \sum_{\sigma s} \delta\sigma_i A_{s\sigma} F_0(s)\, \delta s_j \tag{A3}$$

$$\kappa^{\lambda} \Omega_{ij_1 \cdots j_\lambda}^{(\lambda)} = \sum_{\sigma s} \delta\sigma_i A_{s\sigma} F_0(s)\, \delta s_{j_1}\, \delta s_{j_2} \cdots \delta s_{j_\lambda} \tag{A4}$$

where

$$F_0(s) = \prod_{j=1}^{b} f^{s_j}(1-f)^{1-s_j} = f^{\rho(s)}(1-f)^{b-\rho(s)} \tag{A5}$$

with $\rho(s) = \sum_i s_i$. To obtain the second equality of (A3) the normalization condition $\sum_\sigma A_{s\sigma} = 1$ has been used.

As the FHP models, considered in this paper, are detailed balance models with symmetric transition probabilities $A_{s\sigma} = A_{\sigma s}$, it follows immediately that $\Omega^{(1)}$ is a symmetric matrix if we use in addition particle conservation in the form $A_{\sigma s}\rho(s) = A_{\sigma s}\rho(\sigma)$. The expressions (A3) and (A4) have been used in the body of the paper to obtain (4.12).

ACKNOWLEDGMENTS

The authors would like to thank M. Gerits and M. van der Hoef for making their simulation data available prior to publication. The work of R. B. is sponsored by the DIGICYT (Spain) PB88-0140, Stichting voor Fundamenteel Onderzoek der Materie (FOM), and Universidad Complutense through the program "Bolsas 92."

REFERENCES

1. U. Frisch, D. d'Humières, B. Hasslacher, P. Lallemand, Y. Pomeau, and J. P. Rivet, *Complex Systems* **1**:649 (1987); see also G. D. Doolen, ed., *Lattice Gas Methods for Partial Differential Equations*, reprint volume (Addison-Wesley, 1990), p. 75.
2. D. d'Humières and P. Lallemand, in *Lattice Gas Methods for Partial Differential Equations*, G. D. Doolen, ed., reprint volume (Addison-Wesley, 1990), p. 299.
3. B. Boghosian and C. D. Levermore, in *Discrete Kinetic Theory, Lattice Gas Dynamics and Foundations of Hydrodynamics*, R. Monaco, ed. (World Scientific, Singapore, 1989), p. 44.
4. M. Gerits and M. A. van der Hoef, unpublished (1991).
5. M. A. van der Hoef and D. Frenkel, *Phys. Rev. A* **41**:4277 (1990).
6. J. R. Dorfman and H. van Beijeren, *Statistical Mechanics, Part B: Time-Dependent Processes*, B. J. Berne, ed. (Plenum Press, New York, 1977).
7. T. R. Kirkpatrick and M. H. Ernst, *Phys. Rev. A* **44**:8051 (1991).
8. D. Frenkel and M. H. Ernst, *Phys. Rev. Lett.* **63**:2165 (1989).
9. T. Naitoh, M. H. Ernst, M. A. van der Hoef, and D. Frenkel, *Phys. Rev. A* **44**:2484 (1991); and preprint (1991).
10. M. A. van der Hoef and D. Frenkel, *Phys. Rev. Lett.* **66**:1591 (1991).
11. T. Naitoh, M. H. Ernst, and J. W. Dufty, *Phys. Rev. A* **42**:7187 (1990).
12. J. A. Leegwater and G. Szamel, *Phys. Rev. Lett.* **67**:408 (1991).
13. R. Brito and M. H. Ernst, submitted.
14. M. H. Ernst and J. W. Dufty, *J. Stat. Phys.* **58**:57 (1990).
15. R. Brito, M. H. Ernst, and T. R. Kirkpatrick, *J. Stat. Phys.* **62**:283 (1991).
16. R. Brito and M. H. Ernst, *Phys. Rev. A* **44**:8384 (1991).